



Fates of secondary organic aerosols in the atmosphere identified from compound-specific dual-carbon isotope analysis of oxalic acid

Buqing Xu^{1,2}, Jiao Tang^{1,2}, Tiangang Tang^{1,3}, Shizhen Zhao^{1,2}, Guangcai Zhong^{1,2},
Sanyuan Zhu^{1,2}, Jun Li^{1,2}, Gan Zhang^{1,2*}

¹State Key Laboratory of Organic Geochemistry, Guangzhou Institute of Geochemistry, Chinese Academy of Sciences, Guangzhou 510640, China.

²CAS Center for Excellence in Deep Earth Science, Guangzhou 510640, China

³Key Laboratory of Agro-ecological Processes in Subtropical Region, Institute of Subtropical Agriculture, Chinese Academy of Sciences, Changsha, 410125, China.

*Correspondence: Gan Zhang (zhanggan@gig.ac.cn)



1 **Abstract**

2 Secondary organic aerosols (SOAs) are important components of fine particulates in
3 the atmosphere. However, the sources of SOA precursor and atmospheric processes
4 affecting SOAs are poorly understood. This limits our abilities to improve air quality
5 and model aerosol-mediated climate forcing. Here, we use novel compound-specific
6 dual-carbon isotope fingerprints ($\Delta^{14}\text{C}$ and $\delta^{13}\text{C}$) for dominant SOA tracer molecules
7 (oxalic acid and related polar compounds) to investigate the fates of SOAs in the
8 atmosphere at five emission hotspots in China. Coal combustion and vehicle exhausts
9 accounted for ~55% of the sources of carbon in oxalic acid in Beijing and Shanghai,
10 but biomass-burning and biogenic emissions accounted for ~70% of the sources of
11 carbon in oxalic acid in Chengdu, Guangzhou, and Wuhan. The dual-carbon isotope
12 signatures of SOA molecules and bulk organic carbon pools (e.g., water-soluble organic
13 carbon) were compared to investigate the fates of SOAs in the atmosphere.
14 Photochemical aging of organic aerosols was dominant in summer, but fresh SOA
15 formation from precursor volatile organic compounds was dominant in winter. The
16 results indicated that SOA carbon sources and chemical processes producing SOAs
17 vary spatially and seasonally and these variations need including in Chinese climate
18 projection models and air quality management practices.



19 **1. Introduction**

20 Great efforts have been made to decrease fine particle (PM_{2.5}) pollution in China,
21 which led to a great improvement in air quality during the last decade. However, PM_{2.5}
22 concentrations in Chinese urban areas are still much higher than the World Health
23 Organization guideline (Xing et al., 2020). Further improvements in air quality will be
24 difficult to achieve because primary particulate emissions have already been effectively
25 controlled through stringent regulatory polices established since 2005 (Zhao et al., 2018)
26 and emissions of volatile organic compounds have remained stable (Wang et al., 2021).
27 Field observations have indicated that most organic aerosols in Chinese urban areas are
28 secondary organic aerosols (SOAs) formed through oxidation of biogenic and
29 anthropogenic precursor volatile organic compounds in the atmosphere (Huang et al.,
30 2014). Our poor understanding of SOAs leads to some of the most important
31 uncertainties when assessing global/regional climate forcing, either directly through
32 solar radiation scattering and absorption or indirectly through aerosol–cloud
33 interactions (Carlton et al., 2009; Hallquist et al., 2009). The sources of SOAs and
34 chemical processes affecting SOAs in polluted areas of China need to be better
35 understood to allow air quality control strategies to be optimized and accurate
36 simulations of climate forcing to be developed.

37 The large variety of SOA precursors and the complexity of physical/chemical
38 processes in real atmosphere renders great challenges in understanding SOA formation.
39 Radiocarbon ($\Delta^{14}\text{C}$) measurements of organic aerosol components allow high-precision
40 fingerprinting to be achieved and the relative contributions of fossil fuels and
41 biogenic/biomass sources to be determined (Gustafsson et al., 2009; Zhang et al., 2021).
42 The $\Delta^{14}\text{C}$ values for bulk organic aerosol materials such as black carbon (BC), organic
43 carbon (OC), and water-soluble organic carbon (WSOC) have been determined
44 (Andersson et al., 2015; Szidat et al., 2004; Szidat et al., 2006; Kirillova et al., 2013;
45 Liu et al., 2014), but it is still difficult to directly measure the $\Delta^{14}\text{C}$ values of SOAs in



46 atmospheric aerosols, which are chemically complex. Molecular-level $\Delta^{14}\text{C}$ analysis of
47 SOA markers can overcome this problem and remove uncertainty caused by using
48 bottom-up organic precursor emission inventories (Chang et al., 2022).

49 Oxalic acid is a useful SOA marker because it is a key end-product of various
50 transformation pathways in the atmosphere and is typically the most abundant SOA
51 component (Boreddy and Kawamura, 2018; Kawamura and Bikkina, 2016;
52 Myriokefalitakis et al., 2011). Stable carbon isotope measurements ($\delta^{13}\text{C}$) of oxalic acid
53 have been widely used to differentiate between various atmospheric processes affecting
54 organic aerosols (Aggarwal and Kawamura, 2008; Wang et al., 2020; Zhang et al., 2016;
55 Shen et al., 2022; Qi et al., 2022). Estimated kinetic isotope effects indicate that
56 secondary formation and photochemical aging will affect $\delta^{13}\text{C}$ in opposite ways
57 (Kirillova et al., 2013). Combining $\delta^{13}\text{C}$ and $\Delta^{14}\text{C}$ measurements of oxalic acid could
58 therefore allow the carbon sources of SOAs to be identified and processes affecting
59 SOAs in the ambient atmosphere to be investigated.

60 In this study, we determined the dual-carbon isotope fingerprints ($\Delta^{14}\text{C}$ and $\delta^{13}\text{C}$)
61 of water-soluble SOA components (oxalic acid and related polar organic acids) and their
62 parent water-soluble aerosols (i.e., WSOC) in five highly industrialized and populated
63 megacities in China. The cities were Beijing, Chengdu, Guangzhou, Shanghai, and
64 Wuhan, which were used to represent the five main regional carbon emission hotspots
65 in China (the North China Plain, the Sichuan Basin, the Pearl River Delta, the Yangtze
66 River Delta, and the middle reaches of the Yangtze River, respectively) (Fig. S1). We
67 determined spatial and seasonal variations in the sources of carbon in oxalic acid in the
68 study areas. We then compared the $\delta^{13}\text{C}$ and $\Delta^{14}\text{C}$ data for oxalic acid and the bulk
69 organic aerosol pool to investigate the atmospheric processes affecting SOAs in the
70 different cities and seasons. The molecular-level isotope fingerprints allowed
71 observational constraints on the sources of carbon in SOAs and atmospheric processes
72 affecting SOAs to be determined. The results improve our understanding of the fates of
73 SOAs in the atmosphere.



74 **2 Methods**

75 **2.1 Sampling campaign**

76 Field sampling was performed in five megacities, Beijing, Chengdu, Guangzhou,
77 Shanghai, and Wuhan. The locations of the cities are shown in [Fig. S1](#). Sampling was
78 performed at an urban site and a suburban site in each city so that city-level data were
79 acquired. The sampling campaign was described previously (Zhao et al., 2021) and
80 sampling information is shown in [Table S1](#). At each site, PM_{2.5} samples were collected
81 onto pre-combusted Whatman quartz-fiber filters (20 cm × 25 cm) using a high-volume
82 sampler and a flow rate of 1 m³ min⁻¹. Two intensive sampling campaigns were
83 performed at each sampling site, with consecutive 24 h samples collected for 1 week in
84 January 2018 (winter) and July 2018 (summer). A single sample representing the winter
85 or summer at a sampling site was prepared by combining a one-tenth portion of each
86 filter collected in a sampling campaign at the site. A total of 20 pooled samples were
87 prepared and used in the subsequent experiments. One field blank sample for each site
88 was collected and analyzed. The samples were stored at -20 °C until they were analyzed.

89 **2.2 Extracting water-soluble ions, WSOC, and dicarboxylic acids**

90 Each pooled sample was extracted four times. Each extraction involved adding 50
91 mL of ultrapure water to the sample and ultrasonicated the sample for 30 min. The
92 extracts were combined and passed through a 0.22 μm polytetrafluoroethylene
93 membrane filter. Each extract was divided into several portions of different volumes,
94 and the different portions were analyzed to determine the concentrations and/or carbon
95 isotope compositions of water-soluble ions, WSOC, and dicarboxylic acids.

96 The carbon content of the WSOC was determined using a TOC-VCPH total
97 organic carbon analyzer (Shimadzu, Kyoto, Japan) following the non-purgeable organic
98 carbon analysis method (Kirillova et al., 2010). Water-soluble inorganic ions (Ca²⁺, Cl⁻,
99 K⁺, Mg²⁺, Na⁺, NH₄⁺, NO₃⁻, and SO₄²⁻) were determined using a Metrohm 761
100 Compact IC ion chromatograph (Metrohm, Herisau, Switzerland). The WSOC and



101 water-soluble inorganic ion concentrations in duplicate samples were determined, and
102 the concentrations were corrected for the concentrations in the field blanks (Mo et al.,
103 2021).

104 **2.3 Dicarboxylic acid analysis and carbon isotope analysis**

105 The stable carbon isotope $\delta^{13}\text{C}$ and radiocarbon $\Delta^{14}\text{C}$ values for dicarboxylic acids
106 were determined using previously published methods (Xu et al., 2021). Briefly, an
107 ultrapure water extract of a sample was evaporated to dryness and then derivatized with
108 10% BF_3 in 1-butanol (Sigma-Aldrich, St Louis, MO, USA) at 100 °C for 1 h to convert
109 carboxyl groups into butyl ester groups. The derivatives were extracted with *n*-hexane
110 and quantified by gas chromatography mass spectrometry before isotope analysis was
111 performed. The $\delta^{13}\text{C}$ values for individual diacids were determined by gas
112 chromatography isotope ratio mass spectrometry (Thermo Fisher Scientific Delta V,
113 Waltham, MA, USA). Each sample was analyzed in triplicate and the analytical errors
114 for the replicate analyses were generally <0.3‰.

115 Compound-specific radiocarbon analysis of oxalic acid was achieved by
116 separating and harvesting single compounds using a preparative capillary gas
117 chromatograph in sufficient amounts to allow offline natural abundance ^{14}C
118 measurements to be made by accelerator mass spectrometry. The preparative capillary
119 gas chromatography isolates were rinsed with dichloromethane, completely dried, and
120 combusted at 920 °C with CuO and Ag in a quartz tube to give CO_2 . The CO_2 was
121 purified in a vacuum system and then reduced to graphite using the hydrogen reduction
122 method. The $\Delta^{14}\text{C}$ value was determined using the 1.5 SDH-1, 0.5 MV compact
123 accelerator mass spectrometry facility (NEC, National Electrostatics Corporation, USA)
124 at the Guangzhou Institute of Geochemistry of the Chinese Academy of Sciences (Zhu
125 et al., 2015). Each accelerator mass spectrometry analysis ^{14}C result is reported as a
126 fraction modern (F_m) normalized to a common $\delta^{13}\text{C}$ values of -25‰. The results were
127 corrected for background carbon using an isotope dilution method described in previous
128 publications (Xu et al., 2021). The $\delta^{13}\text{C}$ and F_m values for individual diacids were



129 calculated using the relevant isotope ratios for diacid derivatives and 1-butanol using
130 an isotope mass balance equation. Each F_m result was converted into a “fraction of
131 contemporary carbon” (F_c) by normalizing the F_m using a conversion factor of 1.06 to
132 correct for excess ^{14}C from nuclear bomb tests (Xu et al., 2022).

133 **2.4 Carbon isotope analysis of WSOC**

134 A ~15 mL aliquot of a WSOC extract was cooled to $-20\text{ }^\circ\text{C}$ and dried in a vacuum
135 freeze drier. The residue was redissolved in ~200 μL of ultrapure water, then 50 μL was
136 transferred to a tin capsule for stable carbon isotope analysis and 150 μL was transferred
137 to a capsule for radiocarbon analysis. The samples in the capsules were evaporated to
138 dryness at $60\text{ }^\circ\text{C}$ before isotope analyses were performed.

139 The carbon isotopes in the WSOC were determined using a previously published
140 procedure (Mo et al., 2021). The $\delta^{13}\text{C}$ value for WSOC was determined using a Flash
141 2000 elemental analyzer connected to a Delta V ion ratio mass spectrometer (Thermo
142 Fisher Scientific, Waltham, MA, USA). The $\Delta^{14}\text{C}$ values for the WSOC samples were
143 determined at the accelerator mass spectrometry facility (1.5 SDH-1, 0.5 MV, NEC,
144 USA). Generally, $>200\text{ }\mu\text{g}$ of WSOC were combusted and converted into graphite for
145 each radiocarbon analysis.

146 **3 Results and Discussion**

147 **3.1 Spatiotemporal variations in dicarboxylic acids**

148 Dicarboxylic acid, oxocarboxylic acid, and α -dicarbonyl concentrations in the
149 $\text{PM}_{2.5}$ samples collected in the winter and summer in the five megacities were
150 determined, and a total of 29 water-soluble organic species were identified, as shown
151 in Table S2. The diacid and related compound concentrations were slightly higher at
152 the urban than suburban sites, but the differences were not significant. For each city,
153 the mean of the concentrations found at the urban and suburban sites is therefore
154 presented.

155 The total diacid concentrations in the samples from the five megacities were 25–

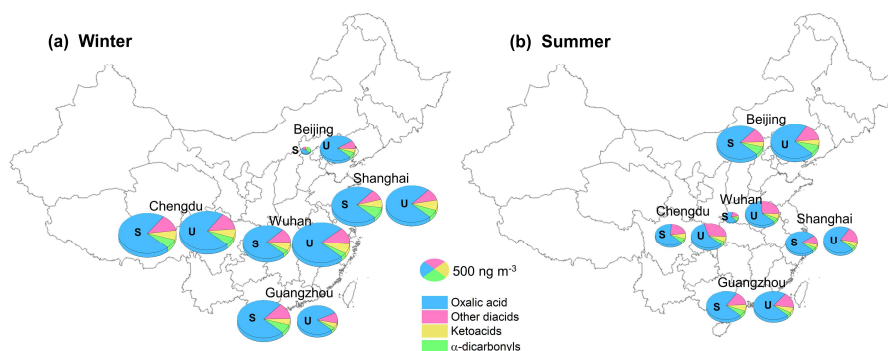


156 1300 ng m⁻³ (mean ± standard deviation 690 ± 360 ng m⁻³), which were similar to
157 concentrations previously found in other Asian megacities such as Chennai (mean 610
158 ng m⁻³) (Pavuluri et al., 2010) and Hong Kong (mean 690 ng m⁻³) (Ho et al., 2006) and
159 slightly lower than concentrations found in 14 Chinese cities in 2003 (890 ± 460 ng
160 m⁻³) (Ho et al., 2007). Oxalic acid was the most abundant diacid at all of the sampling
161 sites and contributed 70%–89% (mean 82%) of the total diacid concentrations. The
162 mean oxalic acid to total diacid concentration ratios were significantly higher than the
163 mean of 58% found for 14 urban sites in China in 2003 (Ho et al., 2007). The increase
164 in the oxalic acid to total diacid concentration ratio between 2003 and 2018 indicated
165 that secondary organic aerosol production in China increased between 2003 and 2018
166 because oxalic acid is an end-product of the oxidation of many precursors (Ervens et
167 al., 2011; Carlton et al., 2007; Lim et al., 2010; Lim et al., 2013). Malonic acid and
168 succinic acid were approximately equally the second most abundant diacids,
169 contributing 4.4% and 4.7%, respectively, of the total diacid concentrations, and
170 phthalic acid, terephthalic acid, adipic acid, and azelaic acid were the next most
171 abundant diacids. The mean oxoacid concentration was 54 ± 34 ng m⁻³, and glyoxylic
172 acid and pyruvic acid were the most and second most abundant oxoacids, respectively.
173 Two α-dicarbonyls (important oxalic acid precursors) were also determined (Fu et al.,
174 2008; Warneck, 2003). Methylglyoxal was more abundant than glyoxal, and this was
175 partly attributed to the rate of oxidation by OH radicals being lower for methylglyoxal
176 than glyoxal (Meng et al., 2018).

177 In Beijing (in North China), the diacid concentration was markedly lower in winter
178 (260 ng m⁻³) than summer (850 ng m⁻³) (Fig. 1), probably because weaker solar
179 radiation and lower temperatures caused less photochemical oxidation to occur in
180 winter than summer (Ho et al., 2007). In particular, during the winter sampling period,
181 clean air masses originating in Siberia dominated the atmosphere in Beijing (Fig. S2)
182 and may have caused the secondary aerosol precursor concentrations to be very low. In
183 contrast, the winter to summer diacid concentration ratios for the cities in South China



184 (Chengdu, Guangzhou, Shanghai, and Wuhan) were >1 (range 1.4–4.2) (Fig. 1). Unlike
185 for Beijing, strong photochemical oxidation would have occurred in winter in the cities
186 in South China (Ho et al., 2007). The diacid concentrations were probably higher in
187 winter than summer because the mixing heights were lower and precipitation was less
188 frequent in winter than summer. Oxocarboxylic acids and α -dicarbonyls had similar
189 spatial and seasonal patterns to diacids, the concentrations being higher in South China
190 in winter than summer but higher in North China in summer than winter.



191

192 **Figure 1.** Dicarboxylic acid, oxocarboxylic acid, and α -dicarbonyl concentrations in
193 $\text{PM}_{2.5}$ collected in five Chinese megacities in (a) winter and (b) summer. Samples were
194 collected at a suburban site (S) and an urban site (U) in each city.

195 3.2 Radiocarbon-based oxalic acid source apportionment

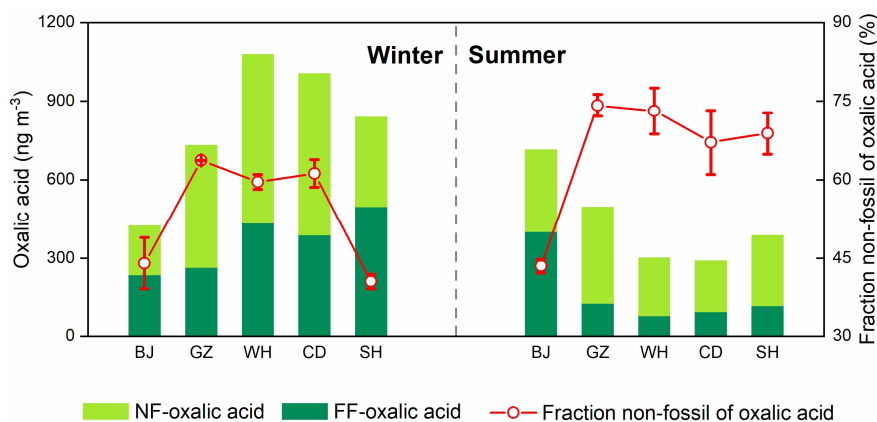
196 We determined the $\Delta^{14}\text{C}$ values for oxalic acid (the most abundant diacid) in the
197 samples. The sources of oxalic acid were apportioned based on the $\Delta^{14}\text{C}$ data, and the
198 non-fossil contributions to the oxalic acid concentrations ($f_{\text{NF-oxalic acid}}$) were 40%–
199 76% (mean $61\% \pm 11\%$), as shown in Table S3. The high proportion of $f_{\text{NF-oxalic acid}}$
200 demonstrates that even in the heavily populated and industrialized areas of China, non-
201 fossil emissions are important and ubiquitous sources of oxalic acid. The important non-
202 fossil sources of oxalic acid may be seasonally produced biogenic precursors and
203 precursors emitted during biomass burning. The $f_{\text{NF-oxalic acid}}$ values were higher for
204 the suburban sites than the urban areas except for Shanghai (Table S3). This is
205 consistent with larger amounts of fossil fuels being consumed in urban areas than



206 suburban areas. However, intraurban differences were not marked, so the $\Delta^{14}\text{C}$ -based
207 source apportionment results for the different cities were compared.

208 The mean f_{NF} -oxalic acid value was higher in summer ($67\% \pm 10\%$) than winter
209 ($54\% \pm 11\%$), indicating that more emissions were caused by fossil fuel combustion
210 and/or less biogenic emissions occurred in winter than summer. In winter, fossil-fuel-
211 derived carbon contributed $\sim 60\%$ of the carbon in oxalic acid in Beijing and Shanghai
212 (Fig. 2) but $<40\%$ of the carbon in oxalic acid in Chengdu, Guangzhou, and Wuhan.
213 This agreed with the results of a previous study in which the sources of SOA during
214 winter haze events were apportioned using two complementary bilinear receptor
215 models and fossil sources were found to contribute 63%, 50%, and 35% of SOAs in
216 Beijing, Shanghai, and Guangzhou, respectively (Huang et al., 2014). Oxalic acid was
217 therefore a good surrogate for SOA.

218 In summer, a mean of $71\% \pm 4\%$ of the oxalic acid in Chengdu, Guangzhou,
219 Shanghai, and Wuhan (in South China) was derived from natural biomass (Fig. 2).
220 However, a large proportion ($56\% \pm 1\%$) of the oxalic acid in Beijing (in North China)
221 was derived from fossil carbon (Fig. 2). Biogenic precursors are expected to be more
222 important in summer than winter, but fossil-fuel-derived carbon contributed most of the
223 oxalic acid in Beijing in both summer and winter. Back trajectories indicated that the
224 air masses in Beijing during the summer sampling periods mostly originated over the
225 Beijing–North China Plain (Fig. S2), which is one of the most polluted parts of China
226 (Andersson et al., 2015; Zhao et al., 2021).



227
228 **Figure 2.** Mass concentrations of oxalic acid derived from non-fossil sources (NF) and
229 fossil fuel (FF) and the proportions of non-fossil oxalic acid found for Beijing (BJ),
230 Guangzhou (GZ), Wuhan (WH), Chengdu (CD), and Shanghai (SH) in winter and
231 summer.

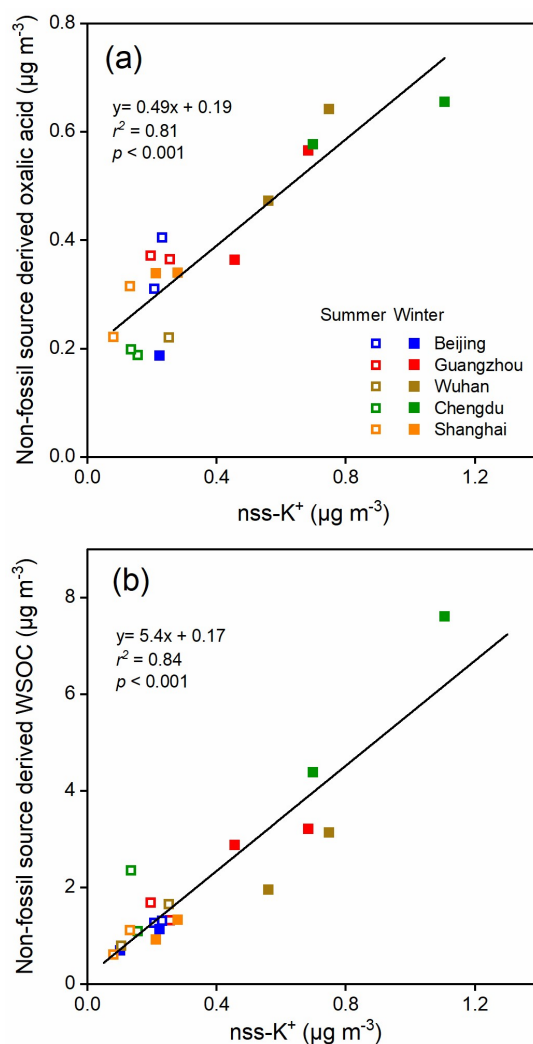
232 The concentrations of oxalic acid derived from non-fossil sources and fossil fuel
233 were 190–660 ng m⁻³ (mean 370 ± 150 ng m⁻³) and 81–520 ng m⁻³ (mean 260 ± 150
234 ng m⁻³), respectively (Fig. 2). In winter, the concentrations of oxalic acid derived from
235 fossil fuel were higher in cities in South China than in Beijing. The concentrations of
236 oxalic acid derived from fossil fuel were markedly lower in summer than winter in the
237 cities in South China but higher in summer than winter in Beijing. In summer, the
238 concentrations of oxalic acid derived from fossil fuel were three–five times higher in
239 Beijing than in the cities in South China (Fig. 2). This would have been caused by
240 seasonally dependent fossil fuel consumption and meteorological conditions, as
241 discussed above.

242 Oxalic acid derived from non-fossil sources made substantial contributions to or
243 even dominated the oxalic acid in the cities we studied (Fig. 2). The concentrations of
244 non-fossil oxalic acid in the cities in South China were higher in winter than summer.
245 However, biogenic compounds (e.g., isoprene (Bikkina et al., 2014; Bikkina et al., 2021)
246 and monoterpene (Link et al., 2021)) may contribute a smaller proportion of non-fossil
247 oxalic acid in winter than summer. The high non-fossil oxalic acid concentrations found



248 in winter may therefore have been caused by local and regional biomass burning. As
249 shown in Fig. 3a, the non-fossil oxalic acid concentrations positively correlated with
250 the concentration of non-sea-salt potassium (nss-K⁺; a marker for biomass burning)
251 ($r^2=0.81$, $p<0.001$), indicating that the high non-fossil oxalic acid concentrations were
252 mainly caused by emissions of precursors through biomass burning. The slope of the
253 regression line fitted to a plot of the non-fossil oxalic acid concentration against the
254 nss-K⁺ concentration (0.49 ± 0.06 ; Fig. 3a) was similar to the slope found in a previous
255 study performed in the Pearl River Delta area in South China (0.55 ± 0.08) (Xu et al.,
256 2022). When the biomass burning contribution was very low (nss-K⁺=0 $\mu\text{g m}^{-3}$), the
257 mean non-fossil oxalic acid concentration (190 ng m^{-3} ; Fig. 3a) was half of the mean
258 total oxalic acid concentration (370 ng m^{-3}). This suggested that biogenic emissions
259 and biomass burning contributed equally to the mean total oxalic acid concentration.

260 Non-fossil oxalic acid and nss-K⁺ were less abundant in all of the cities in summer
261 than winter (Fig. 3a), indicating that most of the non-fossil oxalic acid was produced
262 through biogenic emissions in summer. On average, the non-fossil oxalic acid
263 concentrations in Guangzhou, Wuhan, and Chengdu were 1.3, 2.5, and 3.2 times higher,
264 respectively, in winter than summer (Fig. 3a), mostly because more biomass burning
265 occurs in winter than summer. Less marked seasonal variations in non-fossil oxalic acid
266 concentrations were found for Beijing and Shanghai (Fig. 3a), indicating that biomass
267 burning may produce only a small proportion of the oxalic acid found in these cities.
268 This is consistent with emission control legislation being stricter in Beijing and
269 Shanghai than the other cities, meaning biomass burning activities (e.g., crop residue
270 burning) are effectively controlled in Beijing and Shanghai (Qiu et al., 2016). The
271 oxalic acid sources apportioned using the $\Delta^{14}\text{C}$ data suggested that decreasing the
272 concentrations of precursors derived from fossil fuels could be important for controlling
273 SOA production in Beijing and Shanghai. In contrast, decreasing the concentrations of
274 precursors derived from both fossil fuels and biomass combustion will be required to
275 decrease the SOA concentrations in areas such as Chengdu, Guangzhou, and Wuhan.



276

277 **Figure 3.** Relationships between (a) non-fossil-derived oxalic acid concentrations and
278 non-sea-salt potassium (nss- K^+) concentrations and between (b) non-fossil-derived
279 water-soluble organic carbon (WSOC) concentrations and nss- K^+ concentrations.

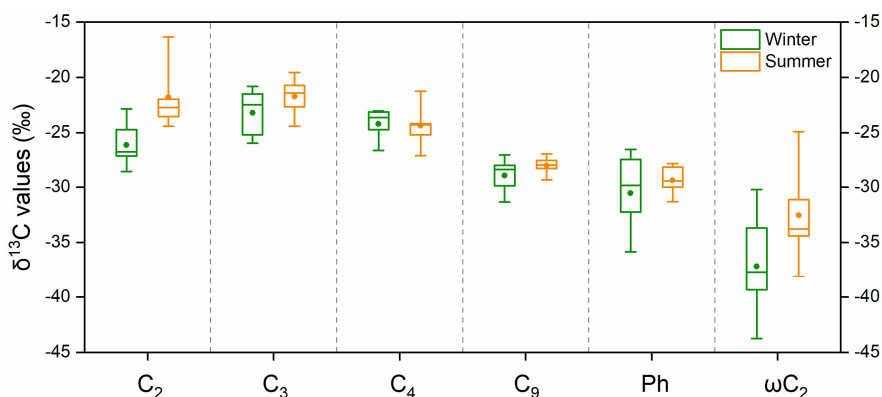
280 3.3 Relationships between stable carbon isotope shifts and atmospheric processing

281 The stable carbon isotope composition ($\delta^{13}\text{C}$) provides useful information about
282 the sources of carbon and particularly about atmospheric processes affecting organic
283 compounds. Primary emissions from various sources have different $\delta^{13}\text{C}$ values. The
284 $\delta^{13}\text{C}$ value will change because of kinetic isotope effects during atmospheric processes



285 (Kirillova et al., 2013) such as oxidation, secondary formation, oligomerization, and
286 gas–particle partitioning (Bikkina et al., 2017b) in which lighter and heavier isotopes
287 behave differently, although source mixing can also affect the $\delta^{13}\text{C}$ value. The $\delta^{13}\text{C}$
288 values of diacids therefore have been used widely to track atmospheric processes and
289 assess the degree of organic aerosol aging (Aggarwal and Kawamura, 2008; Zhang et
290 al., 2016; Wang et al., 2020; Shen et al., 2022; Qi et al., 2022).

291 The $\delta^{13}\text{C}$ values for the main diacids and oxoacids in the five cities that were
292 studied are shown in Fig. 4 and Table S4. Oxalic acid had a markedly lower $\delta^{13}\text{C}$ (by
293 4.4‰) in winter than summer (Fig. 4). This would have been caused by differences in
294 isotope fractionation caused by atmospheric processes in winter and summer,
295 differences in oxalic acid sources in winter and summer, or a combination. The $\delta^{13}\text{C}$
296 values for the diacids with more carbon atoms (C_3 – C_9 diacids) in winter and summer
297 were not very (<1.5‰) different (Fig. 4), so differences in emission sources were not
298 likely to be responsible for the marked seasonal differences in oxalic acid $\delta^{13}\text{C}$ values.
299 The nss- SO_4^{2-} to SO_4^{2-} ratio ($97\% \pm 3\%$) and nss- K^+ to K^+ ratio ($94\% \pm 4\%$) indicated
300 that marine emissions with heavier $\delta^{13}\text{C}$ signatures did not make marked contributions
301 (Dasari et al., 2019) (Fig. S3), particularly in the coastal cities Guangzhou and Shanghai.
302 The seasonal differences in the $\delta^{13}\text{C}$ values could have been stronger for oxalic acid
303 than diacids with more carbon atoms because processes involving isotope fractionation
304 affected diacids with fewer carbon atoms more than diacids with more carbon atoms.
305 The short-chain acid glyoxylic acid is an important precursor of oxalic acid (Bikkina et
306 al., 2017a; Carlton et al., 2007; Lim et al., 2013) that also had markedly different $\delta^{13}\text{C}$
307 values (by 4.7‰) in winter and summer (Fig. 4). The clear seasonal differences in the
308 $\delta^{13}\text{C}$ values for oxalic acid and glyoxylic acid suggested that atmospheric processes
309 markedly affected oxalic acid and glyoxylic acid, which are small molecules.



310

311 **Figure 4.** Box-and-whisker plot of the $\delta^{13}\text{C}$ values for four saturated aliphatic
312 dicarboxylic acids (C_2 , C_3 , C_4 , and C_9), phthalic acid (Ph), and glyoxylic acid (ωC_2) in
313 $\text{PM}_{2.5}$ collected in five Chinese megacities in January 2018 (winter) and July 2018
314 (summer). Each box indicates the median (the line within the box), the mean (the solid
315 dot within the box), the interquartile range (the ends of the box), and the 10th and 90th
316 percentiles (the whiskers).

317 Oxalic acid can be emitted from primary sources, but most oxalic acid in
318 atmospheric aerosol is formed through aqueous-phase reactions and/or photochemical
319 aging, i.e., secondary sources (Huang and Yu, 2007; Van Pinxteren et al., 2014; Xu et
320 al., 2022). During aqueous-phase reactions, water-soluble gas-phase precursors with
321 lower ^{13}C contents will react faster than the same precursors with higher ^{13}C contents,
322 and this will cause the $\delta^{13}\text{C}$ values to be lower for the particulate products than the
323 gaseous reactants (Anderson et al., 2004; Fisseha et al., 2009; Irei et al., 2006). In
324 contrast, photochemical aging processes can give gaseous products (e.g., CO_2 , CO, and
325 volatile organic compounds) which will be enriched in lighter isotopes, causing $\delta^{13}\text{C}$ to
326 be higher for the residual (aged) aerosols than the gaseous oxidation products
327 (Aggarwal and Kawamura, 2008; Pavuluri and Kawamura, 2012).

328 It has been found in several previous studies that aqueous-phase processes play
329 important roles in SOA formation in China in winter (Gkatzelis et al., 2021; Lv et al.,
330 2022; Yu et al., 2021; Wang et al., 2021). This was largely caused by the growth of



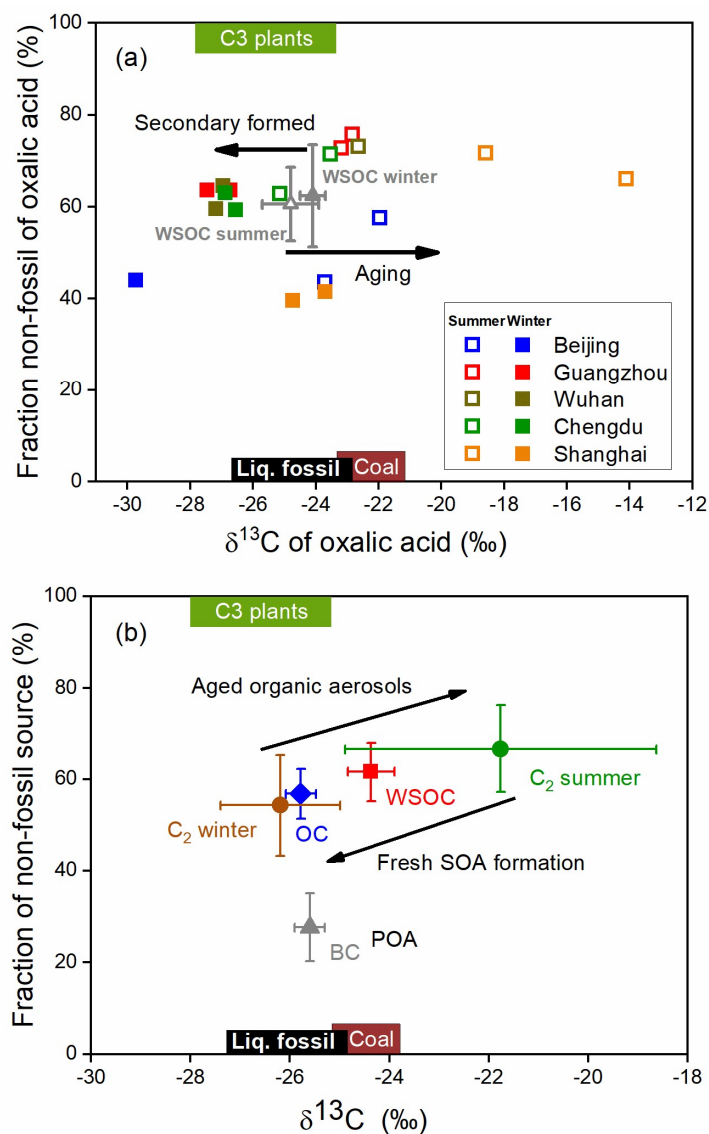
331 aerosol liquid water content (ALWC), because the hygroscopic particles were abundant
332 in winter (Yu et al., 2021; Wang et al., 2020; Chen et al., 2021). Ammonium, nitrate,
333 and sulfate are the most important hygroscopic particles in areas with intense
334 anthropogenic emissions (Wu et al., 2018; Lv et al., 2022). As shown in [Table S5](#), the
335 nitrate concentrations were nine times higher in winter than summer and the ammonium
336 concentrations were 2.5 times higher in winter than summer. The inorganic aerosol
337 (Ca^{2+} , Cl^- , K^+ , Mg^{2+} , Na^+ , NH_4^+ , NO_3^- , and SO_4^{2-}) contents and meteorological
338 parameters (temperature and relative humidity) were used in the ISORROPIA-II
339 thermodynamic model (Xu et al., 2022) and the results indicated that the ALWCs in all
340 five cities were markedly higher in winter ($60 \pm 76 \mu\text{g m}^{-3}$) than summer ($8.5 \pm 5.1 \mu\text{g}$
341 m^{-3}) ([Table S5](#)). The increase in ALWC in winter may facilitate the partitioning of
342 water-soluble organic precursors to the aqueous phase of the aerosol and promote the
343 subsequent formation of low volatile compounds such as oxalic acid in the aqueous
344 phase. Meanwhile, aerosols will be less aged in winter than summer because the
345 temperature is lower and less solar radiation is present in winter than summer.
346 Assuming that source mixing made a minor contribution, the atmospheric processes
347 aging and aqueous SOA formation would have strongly contributed to seasonal
348 variations in the $\delta^{13}\text{C}$ values for oxalic acid in the five Chinese megacities that were
349 studied.

350 **3.4 Tracing sources and aerosol processing using the $\delta^{13}\text{C}$ and $\Delta^{14}\text{C}$ values**

351 Aerosol sources and atmospheric processes affecting aerosols were investigated
352 using the $\delta^{13}\text{C}$ and $\Delta^{14}\text{C}$ values for oxalic acid, as shown in [Fig. 5a](#). As shown in [Fig.](#)
353 [5a](#), the $\delta^{13}\text{C}$ value was higher and the $\Delta^{14}\text{C}$ value indicated more biogenic oxalic acid
354 was present in summer than winter. The oxalic acid data for Chengdu, Guangzhou, and
355 Wuhan strongly overlap in the plot, suggesting that oxalic acid in these cities had similar
356 sources and had been subjected to similar processes. In contrast, the $\delta^{13}\text{C}$ and $\Delta^{14}\text{C}$
357 values for oxalic acid in Beijing and Shanghai are spread over a large area in the plot,
358 indicating that oxalic acid in these cities had various sources and had been subjected to



359 various atmospheric processes. The fossil-carbon contributions to oxalic acid were
 360 markedly higher in Beijing and Shanghai than the other cities, as described above.
 361 However, the $\delta^{13}\text{C}$ values were lower in Beijing and higher in Shanghai. The $\delta^{13}\text{C}$
 362 values suggested that organic aerosols in Beijing were predominantly fresh SOAs but
 363 that organic aerosols were more affected by photochemical aging in Shanghai than the
 364 other cities.



365



366 **Figure 5.** ^{14}C -based non-fossil source fractions plotted against the $\delta^{13}\text{C}$ values for
367 molecules and carbonaceous aerosol components. **(a)** Aerosol oxalic acid collected in
368 Beijing (blue), Guangzhou (red), Wuhan (brown), Chengdu (green), and Shanghai
369 (orange) in summer (open squares) and winter (filled squares). The mean dual carbon
370 isotope signals for water-soluble organic carbon (WSOC) in the five cities in summer
371 (gray open triangles) and winter (gray filled triangles) are also shown (Fig. S4). Each
372 error bar indicates the standard deviation. **(b)** Annual mean values for black carbon (BC,
373 gray triangles), organic carbon (OC, blue diamonds), WSOC (red squares), and oxalic
374 acid (C_2 , brown and green circles) in the five cities (see Table 1 for detailed data and
375 references). Each error bar indicates the standard deviation. Here POA and SOA refer
376 to primary organic aerosol and secondary organic aerosol, respectively. The expected
377 dual carbon signatures for coal, liquid fossil carbon, and C_3 plants were taken from
378 previous publications (Widory et al., 2004; Huang et al., 2006; Kawashima and
379 Haneishi, 2012; Smith and Epstein, 1971; Martinelli et al., 2002; Cao et al., 2011).

380 The mean dual carbon isotope signals for WSOC pool in the five cities were
381 determined and are shown as gray triangles in Fig. 5a for comparison with the signals
382 for oxalic acid. The aging process is more important in summer than winter, but the
383 mean $\delta^{13}\text{C}$ values for WSOC in summer ($-24.8\text{‰} \pm 0.9\text{‰}$) and winter ($-24.1\text{‰} \pm 0.4\text{‰}$)
384 were not markedly different (Fig. S4). The $\Delta^{14}\text{C}$ data for WSOC indicated that the mean
385 non-fossil-carbon contribution to WSOC was $62\% \pm 10\%$ (range 45%–80%; Fig. S4),
386 which was similar to the contribution in 10 Chinese cities in 2013 (mean $60\% \pm 9\%$,
387 range 38%–81%) (Mo et al., 2021). The WSOC concentration was almost twice as high
388 in winter than summer, but the WSOC source patterns in winter and summer were
389 similar (Fig. 5a). As shown in Fig. 3b, the non-fossil WSOC concentration significantly
390 correlated with the biomass burning marker (nss-K^+) concentration ($r^2=0.84$, $p<0.001$).
391 When the biomass burning contribution was very low ($\text{nss-K}^+\approx 0 \mu\text{g m}^{-3}$), the non-fossil
392 WSOC concentration was close to $0 \mu\text{g m}^{-3}$ (Fig. 3b). Unlike oxalic acid, for which
393 biogenic emissions and biomass burning were equally important sources, most of the



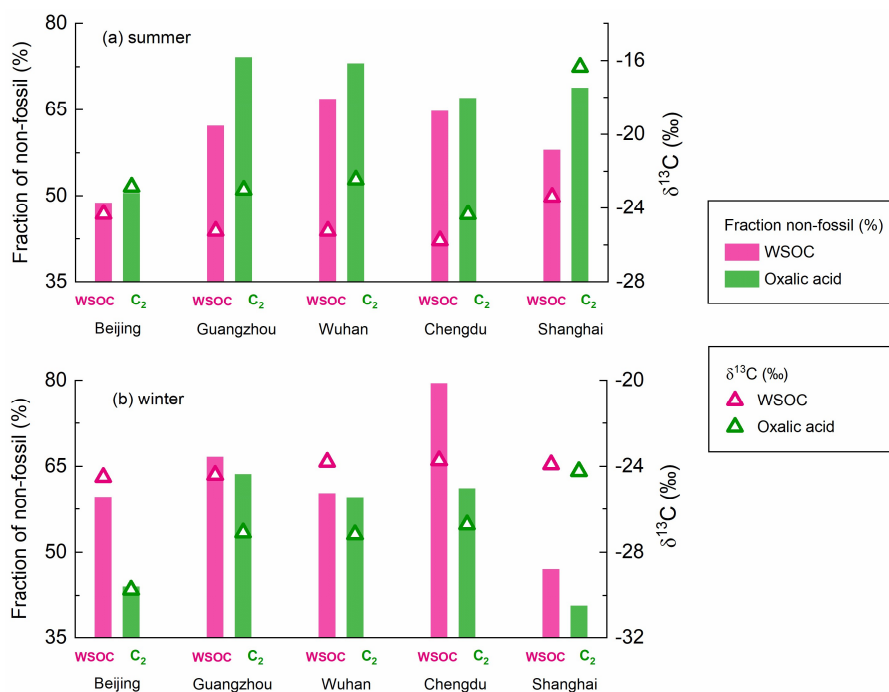
394 non-fossil WSOC was associated with biomass burning. The similar WSOC source
395 patterns in winter and summer were therefore probably caused by fossil fuel
396 combustion and biomass-burning emissions having similar seasonal variations.

397 Oxalic acid contributed a mean of 5.5% (range 1.4%–10.7%) of the WSOC
398 concentration and was probably the most abundant compound (Myriokefalitakis et al.,
399 2011). However, the carbon isotope compositions of oxalic acid and WSOC changed in
400 opposite ways between winter and summer (Fig. 6). This suggested that oxalic acid
401 could have different carbon sources and be affected by different atmospheric processes
402 with the bulk WSOC. The $\delta^{13}\text{C}$ value was higher for oxalic acid than WSOC in summer
403 (Fig. 5a and Fig. 6a), when aerosols are affected by strong photochemical aging
404 processes. It has previously been found that more polar WSOC components are
405 enriched in ^{13}C compared with the total organic carbon in aerosols during
406 photochemical aging (Kirillova et al., 2013; Kirillova et al., 2014a). The larger
407 differences between the $\delta^{13}\text{C}$ values for WSOC and total organic carbon were observed
408 in aerosols which have transported longer distances/times and thereby being more aged
409 during transport. (Kirillova et al., 2014b; Bosch et al., 2014). The $\delta^{13}\text{C}$ value has been
410 found to increase as the number of carbon atoms in diacids decreases (Aggarwal and
411 Kawamura, 2008; Pavuluri et al., 2011), suggesting that shorter-chain diacids, which
412 can form through photochemical aging of longer-chain diacids, will become enriched
413 in ^{13}C during aging. Enrichment of ^{13}C in oxalic acid relative to WSOC (Fig. 6a)
414 therefore probably reflected photochemical aging affecting oxalic acid more than
415 WSOC in summer. The $\Delta^{14}\text{C}$ values indicated more oxalic acid than WSOC was formed
416 from non-fossil carbon in summer (Fig. 6a). This could have been because fossil-carbon
417 components are more recalcitrant than biomass and biogenic components of organic
418 aerosols to oxidative aging (Elmqvist et al., 2006; Kirillova et al., 2014b; Kirillova et
419 al., 2014a), meaning aged oxalic acid (with a higher $\delta^{13}\text{C}$ value) will preferentially form
420 from non-fossil carbon (with a higher $\Delta^{14}\text{C}$ value). As discussed above, biogenic
421 emissions made larger contributions of oxalic acid than WSOC in summer, which gave



422 the same results.

423 In contrast, the $\delta^{13}\text{C}$ values were lower and the $\Delta^{14}\text{C}$ values indicated more oxalic
424 acid than WSOC was formed from fossil carbon in winter (Fig. 5a and Fig. 6b). The
425 lower $\delta^{13}\text{C}$ values for oxalic acid found in winter suggested that oxalic acid was
426 predominantly formed through secondary reactions of gaseous precursors rather than
427 through photochemical aging of aerosols. WSOC aerosols are mixtures of primary
428 organic aerosols (e.g., sugars) and SOAs. Only a small fraction of water-soluble
429 primary organic aerosols would have had fossil fuel sources (Liu et al., 2014; Mo et al.,
430 2021). Therefore, a higher fossil-carbon contribution to water-soluble SOA than WSOC
431 aerosol was expected, and this was indicated by the $\Delta^{14}\text{C}$ values for oxalic acid
432 indicating important fossil-carbon sources. It has been suggested that substantial fossil-
433 carbon-derived precursors are probably oxidized to give water-soluble SOAs through
434 aqueous-phase chemical processes, giving products such as oxalic acid with lower $\delta^{13}\text{C}$
435 values and higher fossil-carbon contributions (Xu et al., 2022). Aqueous-phase
436 processes are facilitated by a high ALWC, which is higher in winter than summer
437 because the hygroscopic particle (e.g., ammonia and nitrate) mass is higher in winter
438 than summer (Lv et al., 2022; Xu et al., 2022) and meteorological conditions (e.g., the
439 boundary layer height, temperature, and wind speed) are unfavorable in winter
440 (Gkatzelis et al., 2021). Photochemical aging is suppressed in winter because of lower
441 temperatures and weaker solar radiation than in summer. This means that more
442 aqueous-phase production of fresh SOA than aerosol photochemical aging will occur
443 in urban areas in China in winter.



444

445 **Figure 6.** Proportions of non-fossil sources (determined from the ^{14}C values) and $\delta^{13}\text{C}$
446 values for water-soluble organic carbon (WSOC) and oxalic acid (C_2) in Beijing,
447 Guangzhou, Wuhan, Chengdu, and Shanghai in (a) summer and (b) winter.

448 3.5. Comparison with carbonaceous aerosol components

449 The $\delta^{13}\text{C}$ and $\Delta^{14}\text{C}$ values for oxalic acid were compared with the mean annual
450 isotope compositions of the bulk carbonaceous aerosols (i.e., BC, OC, and WSOC) in
451 $\text{PM}_{2.5}$ found in the five study areas in previous studies (Fig. 5b and Table 1). Non-fossil-
452 source-derived carbon was the dominant contributor of OC and WSOC aerosols, the
453 mean annual contributions being $57\% \pm 5\%$ and $62\% \pm 6\%$, respectively (Fig. 5b). The
454 large contribution of non-fossil carbon to OC and WSOC (a sub-fraction of OC)
455 contrasted strongly with the large contribution of fossil carbon ($72\% \pm 7\%$) to BC (Fig.
456 5b). This was probably because OC aerosols are more affected than BC by biogenic
457 emissions and biomass burning.

458 The $\delta^{13}\text{C}$ values were higher and the $\Delta^{14}\text{C}$ values indicated smaller contributions
459 of fossil carbon for WSOC than OC in both winter and summer (Fig. 5b). Similar results



460 have been found at other locations and for different aerosol sizes (Kirillova et al., 2013;
461 Kirillova et al., 2014a; Kirillova et al., 2014b; Bosch et al., 2014), and this was
462 explained by atmospheric aging affecting water-soluble organic aerosols more than
463 organic aerosols. SOA formation typically causes $\delta^{13}\text{C}$ to decrease, so fresh secondary
464 production of WSOC from fossil carbon would be less likely. However, the sources and
465 processes affecting the different aerosol components were masked in the mean isotope
466 contents of the aerosol mixtures. Oxalic acid is one of the most abundant compounds
467 in WSOC aerosols. The $\delta^{13}\text{C}$ values were lower for the oxalic acid than the WSOC and
468 the $\Delta^{14}\text{C}$ values indicated that fossil carbon made larger contributions to the oxalic acid
469 than the WSOC aerosol in winter (Fig. 5b). This indicated that water-soluble SOA was
470 predominantly produced from fossil-fuel-derived carbon in the study areas in winter.
471 The marked differences between the different organic aerosol components indicated
472 that dual-carbon-isotope studies of more aerosol molecules and components should be
473 performed to improve our understanding of the origins and evolution of organic
474 aerosols in the atmosphere.

475 **Table 1.** Compilation of literature values of $\delta^{13}\text{C}$ compositions and ^{14}C -based non-fossil
476 source fraction (f_{NF}) for black carbon (BC), organic carbon (OC), water-soluble organic
477 carbon (WSOC), and oxalic acid in $\text{PM}_{2.5}$ samples collected from Beijing, Shanghai,
478 Guangzhou, Chengdu, and Wuhan.

Components	Location	Season	$\delta^{13}\text{C}$ (‰)	f_{NF} (%)	References
BC	Beijing	Annual	NA ^a	21	(Zhang et al., 2015)
	Beijing	Annual	NA	18	(Zhang et al., 2017)
	Beijing	Annual	-24.6	24	(Fang et al., 2018)
	Beijing	Summer/winter	-25.8	NA	(Cao et al., 2011)
	Shanghai	Summer/winter	-25.9	NA	(Cao et al., 2011)
	Shanghai	Annual	-25.6	30	(Fang et al., 2018)
	Guangzhou	Summer/winter	-25.9	NA	(Cao et al., 2011)
	Guangzhou	Annual	-25.3	25	(Fang et al., 2018)
	Chengdu	Annual	-26.1	41	(Fang et al., 2018)
	Wuhan	Summer/winter	-25.4	NA	(Cao et al., 2011)
	Wuhan	Winter	NA	26	(Liu et al., 2016b)
	Average		-25.6±0.3	28±7	
OC	Beijing	Summer/winter	-26.0	NA	(Cao et al., 2011)
	Beijing	Annual	NA	52	(Zhang et al., 2017)



	Beijing	Annual	NA	50	(Liu et al., 2020)
	Shanghai	Summer/winter	-25.8	NA	(Cao et al., 2011)
	Shanghai	Winter	NA	51	(Huang et al., 2014)
	Shanghai	Annual	NA	53	(Liu et al., 2020)
	Guangzhou	Summer/winter	-26	NA	(Cao et al., 2011)
	Guangzhou	Annual	NA	55	(Liu et al., 2020)
	Guangzhou	Spring	NA	54	(Liu et al., 2016a)
	Chengdu	autumn	NA	73	(Liu et al., 2017)
	Wuhan	Summer/winter	-25.6	NA	(Cao et al., 2011)
	Wuhan	Winter	NA	62	(Liu et al., 2016b)
	Wuhan	Autumn	NA	66	(Liu et al., 2017)
	Average		-25.9±0.3	57±5	
	Beijing	Summer/winter	-24.4	55	This work
	Shanghai	Summer/winter	-23.6	53	This work
	Guangzhou	Summer/winter	-24.8	63	This work
	Chengdu	Summer/winter	-24.7	72	This work
	Wuhan	Summer/winter	-23.6	65	This work
WSOC	Beijing	Annual	-23.7	56	(Mo et al., 2021)
	Shanghai	Annual	-24	58	(Mo et al., 2021)
	Guangzhou	Annual	-24.7	59	(Mo et al., 2021)
	Chengdu	Annual	-24.9	69	(Mo et al., 2021)
	Wuhan	Annual	-24.3	67	(Mo et al., 2021)
	Average		-24.4±0.5	62±6	
	Beijing	Summer	-22.8	50.5	This work
	Shanghai	Summer	-16.3	68.8	This work
	Guangzhou	Summer	-23	74.2	This work
	Chengdu	Summer	-24.3	67.1	This work
	Wuhan	Summer	-22.4	73.1	This work
Oxalic acid	Beijing	Winter	-25.8	44.1	This work
	Shanghai	Winter	-24.2	40.6	This work
	Guangzhou	Winter	-27.1	63.7	This work
	Chengdu	Winter	-26.7	61.2	This work
	Wuhan	Winter	-27.1	62.1	This work
	Average	Summer	-21.8±3.1	67±10	
	Average	Winter	-26.2±1.2	54±11	

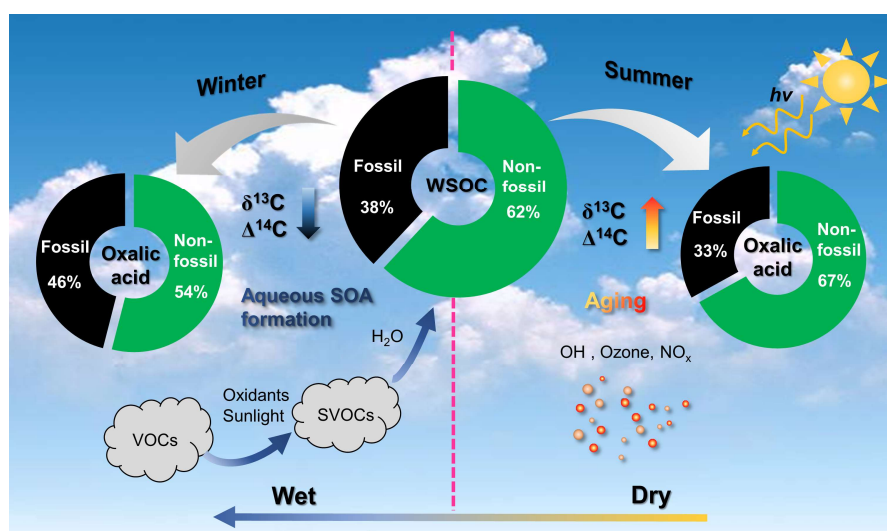
479 ^a NA: no data

480 **4 Conclusions**

481 The $\Delta^{14}\text{C}$ and $\delta^{13}\text{C}$ values of oxalic acid in five megacities in China gave valuable
 482 information about the sources of carbon in SOAs and atmospheric processes affecting
 483 SOAs. The method allowed the fates of SOA in the atmosphere in urban areas to be
 484 investigated even though SOAs are very complex. The SOA sources apportioned from
 485 the ^{14}C values indicated marked seasonal variations, non-fossil carbon being dominant



486 in summer and fossil carbon and non-fossil carbon making similar contributions in
487 winter. Precursors containing fossil carbon emitted through coal combustion or by
488 vehicles were mostly responsible for SOA formation in Beijing and Shanghai. SOA
489 formation was mainly associated with precursors containing non-fossil carbon emitted
490 through biomass burning and/or biogenic emissions in Chengdu, Guangzhou, and
491 Wuhan.



492
493 **Figure 7.** Schematic of the atmospheric fates of secondary organic aerosols (SOAs) in
494 winter and summer. VOCs means volatile organic compounds, SVOCs means semi-
495 volatile organic compounds, and WSOC means water-soluble organic carbon.

496 The dual-carbon-isotope datasets for the individual SOA molecules and bulk
497 organic aerosols indicated that there were two opposite seasonal organic aerosol
498 evolution processes. The fates of SOAs in the atmosphere in winter and summer are
499 shown in Fig. 7. In winter, the high hygroscopic particle mass and unfavorable
500 meteorological conditions (low temperature and high humidity) increase aerosol liquid
501 water formation, which causes fossil-derived water-soluble gaseous organic precursors
502 to dissolve in the aerosol liquid water and aqueous SOA to form (Fig. 7). Oxalic acid
503 indicates freshly formed aqueous SOA in winter because the $\delta^{13}\text{C}$ values were lower
504 for oxalic acid than WSOC and the contribution of fossil carbon was higher for oxalic



505 acid than WSOC. In summer, organic aerosols are more affected by photochemical
506 aging than fresh SOA formation because of the high temperature and the high amount
507 of solar radiation present (Fig. 7). Oxalic acid was affected by SOA aging in summer
508 and the $\delta^{13}\text{C}$ and $\Delta^{14}\text{C}$ values were higher for oxalic acid than WSOC.

509 Overall, we found that the carbon sources and SOA evolution processes were
510 markedly different in different cities and seasons. There is a need to include the large
511 spatial and seasonal variations in SOA fates (including precursor sources, SOA
512 formation through gas-phase oxidation and from aqueous-phase chemicals, and SOA
513 aging) in climate projection models and air quality management in China.

514 **Data availability.** The data underlying the findings of this study are available in this
515 article and its Supplementary Information. The derived data generated in this research
516 will be shared on reasonable request to the corresponding author (GZ).

517 **Author contributions.** GZ and BX designed the study. GCZ and SZZ provided the
518 samples. BX, JT and SYZ carried out the measurements. BX processed data and wrote
519 the paper. GZ, TT, and JL commented on the manuscript.

520 **Competing interests.** The authors declare no competing interests.

521 **Acknowledgements.** We thank Gareth Thomas, PhD, from Liwen Bianji (Edanz)
522 (<https://www.liwenbianji.cn>), for editing the language of a draft of this manuscript.

523 **Financial support.** This work was funded by the Natural Science Foundation of China
524 (42030715), the Alliance of International Science Organizations research and
525 cooperative projects (ANSO-CR-KP-2021-05), the Natural Science Foundation of
526 Guangdong Province, China (2022A1515011679), and the National Key R&D Program
527 of China (2017YFC0212000).

528 **References**

529 Aggarwal, S. G. and Kawamura, K.: Molecular distributions and stable carbon isotopic



- 530 compositions of dicarboxylic acids and related compounds in aerosols from Sapporo, Japan:
531 Implications for photochemical aging during long-range atmospheric transport, *J. Geophys.*
532 *Res.: Atmos.*, 113, 10.1029/2007jd009365, 2008.
- 533 Anderson, R. S., Huang, L., Iannone, R., Thompson, A. E., and Rudolph, J.: Carbon Kinetic Isotope
534 Effects in the Gas Phase Reactions of Light Alkanes and Ethene with the OH Radical at $296 \pm$
535 4 K, *J. Phys. Chem. A*, 108, 11537-11544, 10.1021/jp0472008, 2004.
- 536 Andersson, A., Deng, J., Du, K., Zheng, M., Yan, C., Skold, M., and Gustafsson, O.: Regionally-
537 varying combustion sources of the January 2013 severe haze events over eastern China, *Environ.*
538 *Sci. Technol.*, 49, 2038-2043, 10.1021/es503855e, 2015.
- 539 Bikkina, S., Kawamura, K., and Sarin, M.: Secondary organic aerosol formation over coastal ocean:
540 inferences from atmospheric water-soluble low molecular weight organic compounds, *Environ.*
541 *Sci. Technol.*, 51, 4347-4357, 10.1021/acs.est.6b05986, 2017a.
- 542 Bikkina, S., Kawamura, K., Miyazaki, Y., and Fu, P.: High abundances of oxalic, azelaic, and
543 glyoxylic acids and methylglyoxal in the open ocean with high biological activity: Implication
544 for secondary OA formation from isoprene, *Geophys. Res. Lett.*, 41, 3649-3657,
545 10.1002/2014gl059913, 2014.
- 546 Bikkina, S., Kawamura, K., Sakamoto, Y., and Hirokawa, J.: Low molecular weight dicarboxylic
547 acids, oxocarboxylic acids and α -dicarbonyls as ozonolysis products of isoprene: Implication
548 for the gaseous-phase formation of secondary organic aerosols, *Sci. Total Environ.*, 769, 144472,
549 <https://doi.org/10.1016/j.scitotenv.2020.144472>, 2021.
- 550 Bikkina, S., Andersson, A., Ram, K., Sarin, M. M., Sheesley, R. J., Kirillova, E. N., Rengarajan, R.,
551 Sudheer, A. K., and Gustafsson, Ö.: Carbon isotope-constrained seasonality of carbonaceous
552 aerosol sources from an urban location (Kanpur) in the Indo-Gangetic Plain, *J. Geophys. Res.:*
553 *Atmos.*, 122, 4903-4923, 10.1002/2016jd025634, 2017b.
- 554 Boreddy, S. K. R. and Kawamura, K.: Investigation on the hygroscopicity of oxalic acid and
555 atmospherically relevant oxalate salts under sub- and supersaturated conditions, *Environ. Sci.:*
556 *Processes Impacts*, 20, 1069-1080, 10.1039/c8em00053k, 2018.
- 557 Bosch, C., Andersson, A., Kirillova, E. N., Budhavant, K., Tiwari, S., Praveen, P. S., Russell, L. M.,
558 Beres, N. D., Ramanathan, V., and Gustafsson, Ö.: Source-diagnostic dual-isotope composition
559 and optical properties of water-soluble organic carbon and elemental carbon in the South Asian
560 outflow intercepted over the Indian Ocean, *J. Geophys. Res.: Atmos.*, 119, 7117-7127, 2014.
561 10.1002/2014jd022127, 2014.
- 562 Cao, J.-j., Chow, J. C., Tao, J., Lee, S.-c., Watson, J. G., Ho, K.-f., Wang, G.-h., Zhu, C.-s., and Han,
563 Y.-m.: Stable carbon isotopes in aerosols from Chinese cities: Influence of fossil fuels, *Atmos.*
564 *Environ.*, 45, 1359-1363, <https://doi.org/10.1016/j.atmosenv.2010.10.056>, 2011.
- 565 Carlton, A. G., Wiedinmyer, C., and Kroll, J. H.: A review of Secondary Organic Aerosol (SOA)
566 formation from isoprene, *Atmos. Chem. Phys.*, 9, 4987-5005, 10.5194/acpd-9-8261-2009, 2009.
- 567 Carlton, A. G., Turpin, B. J., Altieri, K. E., Seitzinger, S., Reff, A., Lim, H.-J., and Ervens, B.:
568 Atmospheric oxalic acid and SOA production from glyoxal: Results of aqueous photooxidation
569 experiments, *Atmos. Environ.*, 41, 7588-7602, <https://doi.org/10.1016/j.atmosenv.2007.05.035>,
570 2007.
- 571 Chang, X., Zhao, B., Zheng, H., Wang, S., Cai, S., Guo, F., Gui, P., Huang, G., Wu, D., Han, L.,



- 572 Xing, J., Man, H., Hu, R., Liang, C., Xu, Q., Qiu, X., Ding, D., Liu, K., Han, R., Robinson, A.
573 L., and Donahue, N. M.: Full-volatility emission framework corrects missing and
574 underestimated secondary organic aerosol sources, *One Earth*, 5, 403-412,
575 <https://doi.org/10.1016/j.oneear.2022.03.015>, 2022.
- 576 Chen, Y., Guo, H., Nah, T., Tanner, D. J., Sullivan, A. P., Takeuchi, M., Gao, Z., Vasilakos, P., Russell,
577 A. G., Baumann, K., Huey, L. G., Weber, R. J., and Ng, N. L.: Low-Molecular-Weight
578 Carboxylic Acids in the Southeastern U.S.: Formation, Partitioning, and Implications for
579 Organic Aerosol Aging, *Environ. Sci. Technol.*, 55, 6688-6699, 10.1021/acs.est.1c01413, 2021.
- 580 Dasari, S., Andersson, A., Bikkina, S., Holmstrand, H., Budhavant, K., Satheesh, S., Asmi, E., Kesti,
581 J., Backman, J., Salam, A., Bisht, D. S., Tiwari, S., Hameed, Z., and Gustafsson, Ö.:
582 Photochemical degradation affects the light absorption of water-soluble brown carbon in the
583 South Asian outflow, *Sci. Adv.*, 5, eaau8066, 10.1126/sciadv.aau8066, 2019.
- 584 Elmquist, M., Cornelissen, G., Kukulska, Z., and Gustafsson, O.: Distinct oxidative stabilities of
585 char versus soot black carbon: Implications for quantification and environmental recalcitrance,
586 *Global Biogeochem. Cycles*, 20, 10.1029/2005gb002629, 2006.
- 587 Ervens, B., Turpin, B. J., and Weber, R. J.: Secondary organic aerosol formation in cloud droplets
588 and aqueous particles (aqSOA): a review of laboratory, field and model studies, *Atmos. Chem.*
589 *Phys.*, 11, 11069-11102, 10.5194/acp-11-11069-2011, 2011.
- 590 Fang, W., Du, K., Andersson, A., Xing, Z., Cho, C., Kim, S.-W., Deng, J., and Gustafsson, Ö.: Dual-
591 Isotope Constraints on Seasonally Resolved Source Fingerprinting of Black Carbon Aerosols
592 in Sites of the Four Emission Hot Spot Regions of China, *J. Geophys. Res.: Atmos.*, 123,
593 11,735-711,747, 10.1029/2018jd028607, 2018.
- 594 Fisseha, R., Spahn, H., Wegener, R., Hohaus, T., Brasse, G., Wissel, H., Tillmann, R., Wahner, A.,
595 Koppmann, R., and Kiendler-Scharr, A.: Stable carbon isotope composition of secondary
596 organic aerosol from β -pinene oxidation, *J. Geophys. Res.: Atmos.*, 114, 10.1029/2008jd011326,
597 2009.
- 598 Fu, T.-M., Jacob, D. J., Wittrock, F., Burrows, J. P., Vrekoussis, M., and Henze, D. K.: Global
599 budgets of atmospheric glyoxal and methylglyoxal, and implications for formation of secondary
600 organic aerosols, *J. Geophys. Res.: Atmos.*, 113, 10.1029/2007jd009505, 2008.
- 601 Gkatzelis, G. I., Papanastasiou, D. K., Karydis, V. A., Hohaus, T., Liu, Y., Schmitt, S. H., Schlag, P.,
602 Fuchs, H., Novelli, A., Chen, Q., Cheng, X., Broch, S., Dong, H., Holland, F., Li, X., Liu, Y.,
603 Ma, X., Reimer, D., Rohrer, F., Shao, M., Tan, Z., Taraborrelli, D., Tillmann, R., Wang, H.,
604 Wang, Y., Wu, Y., Wu, Z., Zeng, L., Zheng, J., Hu, M., Lu, K., Hofzumahaus, A., Zhang, Y.,
605 Wahner, A., and Kiendler-Scharr, A.: Uptake of water-soluble gas-phase oxidation products
606 drives organic particulate pollution in Beijing, *Geophys. Res. Lett.*, 48, e2020GL091351,
607 <https://doi.org/10.1029/2020GL091351>, 2021.
- 608 Gustafsson, Ö., Kruså, M., Zencak, Z., Sheesley, R. J., Granat, L., Engström, E., Praveen, P. S., Rao,
609 P. S. P., Leck, C., and Rodhe, H.: Brown Clouds over South Asia: Biomass or Fossil Fuel
610 Combustion, *Science*, 323, 495-498, 10.1126/science.1164857, 2009.
- 611 Hallquist, M., Wenger, J. C., Baltensperger, U., Rudich, Y., Simpson, D., Claeys, M., Dommen, J.,
612 Donahue, N. M., George, C., Goldstein, A. H., Hamilton, J. F., Herrmann, H., Hoffmann, T.,
613 Iinuma, Y., Jang, M., Jenkin, M. E., Jimenez, J. L., Kiendler-Scharr, A., Maenhaut, W.,



- 614 McFiggans, G., Mentel, T. F., Monod, A., Prevot, A. S. H., Seinfeld, J. H., Surratt, J. D.,
615 Szmigielski, R., and Wildt, J.: The formation, properties and impact of secondary organic
616 aerosol: current and emerging issues, *Atmos. Chem. Phys.*, 9, 5155-5236, 10.5194/acp-9-5155-
617 2009, 2009.
- 618 Ho, K. F., Cao, J. J., Lee, S. C., Kawamura, K., Zhang, R. J., Chow, J. C., and Watson, J. G.:
619 Dicarboxylic acids, ketocarboxylic acids, and dicarbonyls in the urban atmosphere of China, *J.*
620 *Geophys. Res.: Atmos.*, 112, 10.1029/2006JD008011, 2007.
- 621 Ho, K. F., Lee, S. C., Cao, J. J., Kawamura, K., Watanabe, T., Cheng, Y., and Chow, J. C.:
622 Dicarboxylic acids, ketocarboxylic acids and dicarbonyls in the urban roadside area of Hong
623 Kong, *Atmos. Environ.*, 40, 3030-3040, 10.1016/j.atmosenv.2005.11.069, 2006.
- 624 Huang, L., Brook, J. R., Zhang, W., Li, S. M., Graham, L., Ernst, D., Chivulescu, A., and Lu, G.:
625 Stable isotope measurements of carbon fractions (OC/EC) in airborne particulate: A new
626 dimension for source characterization and apportionment, *Atmos. Environ.*, 40, 2690-2705,
627 <https://doi.org/10.1016/j.atmosenv.2005.11.062>, 2006.
- 628 Huang, R.-J., Zhang, Y., Bozzetti, C., Ho, K.-F., Cao, J.-J., Han, Y., Daellenbach, K. R., Slowik, J.
629 G., Platt, S. M., Canonaco, F., Zotter, P., Wolf, R., Pieber, S. M., Bruns, E. A., Crippa, M.,
630 Ciarelli, G., Piazzalunga, A., Schwikowski, M., Abbazade, G., Schnelle-Kreis, J.,
631 Zimmermann, R., An, Z., Szidat, S., Baltensperger, U., El Haddad, I., and Prevot, A. S. H.: High
632 secondary aerosol contribution to particulate pollution during haze events in China, *Nature*, 514,
633 218-222, 10.1038/nature13774, 2014.
- 634 Huang, X.-F. and Yu, J. Z.: Is vehicle exhaust a significant primary source of oxalic acid in ambient
635 aerosols?, *Geophys. Res. Lett.*, 34, 10.1029/2006gl028457, 2007.
- 636 Irei, S., Huang, L., Collin, F., Zhang, W., Hastie, D., and Rudolph, J.: Flow reactor studies of the
637 stable carbon isotope composition of secondary particulate organic matter generated by OH-
638 radical-induced reactions of toluene, *Atmos. Environ.*, 40, 5858-5867,
639 <https://doi.org/10.1016/j.atmosenv.2006.05.001>, 2006.
- 640 Kawamura, K. and Bikkina, S.: A review of dicarboxylic acids and related compounds in
641 atmospheric aerosols: Molecular distributions, sources and transformation, *Atmos. Res.*, 170,
642 140-160, 10.1016/j.atmosres.2015.11.018, 2016.
- 643 Kawashima, H. and Haneishi, Y.: Effects of combustion emissions from the Eurasian continent in
644 winter on seasonal $\delta^{13}\text{C}$ of elemental carbon in aerosols in Japan, *Atmos. Environ.*, 46, 568-
645 579, 10.1016/j.atmosenv.2011.05.015, 2012.
- 646 Kirillova, E. N., Sheesley, R. J., Andersson, A., and Gustafsson, Ö.: Natural abundance ^{13}C and
647 ^{14}C analysis of water-soluble organic carbon in atmospheric aerosols, *Anal. Chem.*, 82, 7973,
648 2010.
- 649 Kirillova, E. N., Andersson, A., Han, J., Lee, M., and Gustafsson, Ö.: Sources and light absorption
650 of water-soluble organic carbon aerosols in the outflow from northern China, *Atmos. Chem.*
651 *Phys.*, 14, 1413-1422, 10.5194/acp-14-1413-2014, 2014a.
- 652 Kirillova, E. N., Andersson, A., Tiwari, S., Srivastava, A. K., Bisht, D. S., and Gustafsson, O.: Water-
653 soluble organic carbon aerosols during a full New Delhi winter: Isotope-based source
654 apportionment and optical properties, *J. Geophys. Res.: Atmos.*, 119, 3476-3485,
655 10.1002/2013jd020041, 2014b.



- 656 Kirillova, E. N., Andersson, A., Sheesley, R. J., Krusá, M., Praveen, P. S., Budhavant, K., Safai, P.
657 D., Rao, P. S. P., and Gustafsson, Ö.: 13C- and 14C-based study of sources and atmospheric
658 processing of water-soluble organic carbon (WSOC) in South Asian aerosols, *J. Geophys. Res.:*
659 *Atmos.*, 118, 614-626, 10.1002/jgrd.50130, 2013.
- 660 Lim, Y. B., Tan, Y., and Turpin, B. J.: Chemical insights, explicit chemistry, and yields of secondary
661 organic aerosol from OH radical oxidation of methylglyoxal and glyoxal in the aqueous phase,
662 *Atmos. Chem. Phys.*, 13, 8651-8667, 10.5194/acp-13-8651-2013, 2013.
- 663 Lim, Y. B., Tan, Y., Perri, M. J., Seitzinger, S. P., and Turpin, B. J.: Aqueous chemistry and its role
664 in secondary organic aerosol (SOA) formation, *Atmos. Chem. Phys.*, 10, 10521-10539,
665 10.5194/acp-10-10521-2010, 2010.
- 666 Link, M. F., Brophy, P., Fulgham, S. R., Murschell, T., and Farmer, D. K.: Isoprene versus
667 Monoterpenes as Gas-Phase Organic Acid Precursors in the Atmosphere, *ACS Earth Space*
668 *Chem.*, 5, 1600-1612, 10.1021/acearthspacechem.1c00093, 2021.
- 669 Liu, D., Li, J., Cheng, Z., Zhong, G., Zhu, S., Ding, P., Shen, C., Tian, C., Chen, Y., Zhi, G., and
670 Zhang, G.: Sources of non-fossil-fuel emissions in carbonaceous aerosols during early winter
671 in Chinese cities, *Atmos. Chem. Phys.*, 17, 11491-11502, 10.5194/acp-17-11491-2017, 2017.
- 672 Liu, D., Vonwiller, M., Li, J., Liu, J., Szidat, S., Zhang, Y., Tian, C., Chen, Y., Cheng, Z., Zhong, G.,
673 Fu, P., and Zhang, G.: Fossil and Non-fossil Fuel Sources of Organic and Elemental
674 Carbonaceous Aerosol in Beijing, Shanghai, and Guangzhou: Seasonal Carbon Source
675 Variation, *Aerosol Air Qual. Res.*, 20, 2495-2506, 10.4209/aaqr.2019.12.0642, 2020.
- 676 Liu, J., Li, J., Liu, D., Ding, P., Shen, C., Mo, Y., Wang, X., Luo, C., Cheng, Z., Szidat, S., Zhang,
677 Y., Chen, Y., and Zhang, G.: Source apportionment and dynamic changes of carbonaceous
678 aerosols during the haze bloom-decay process in China based on radiocarbon and organic
679 molecular tracers, *Atmos. Chem. Phys.*, 16, 2985-2996, 10.5194/acp-16-2985-2016, 2016a.
- 680 Liu, J., Li, J., Zhang, Y., Liu, D., Ding, P., Shen, C., Shen, K., He, Q., Ding, X., Wang, X., Chen, D.,
681 Szidat, S., and Zhang, G.: Source apportionment using radiocarbon and organic tracers for
682 PM_{2.5} carbonaceous aerosols in Guangzhou, South China: contrasting local- and regional-scale
683 haze events, *Environ. Sci. Technol.*, 48, 12002-12011, 10.1021/es503102w, 2014.
- 684 Liu, J., Li, J., Vonwiller, M., Liu, D., Cheng, H., Shen, K., Salazar, G., Agrios, K., Zhang, Y., He,
685 Q., Ding, X., Zhong, G., Wang, X., Szidat, S., and Zhang, G.: The importance of non-fossil
686 sources in carbonaceous aerosols in a megacity of central China during the 2013 winter haze
687 episode: A source apportionment constrained by radiocarbon and organic tracers, *Atmos.*
688 *Environ.*, 144, 60-68, 10.1016/j.atmosenv.2016.08.068, 2016b.
- 689 Lv, S., Wang, F., Wu, C., Chen, Y., Liu, S., Zhang, S., Li, D., Du, W., Zhang, F., Wang, H., Huang,
690 C., Fu, Q., Duan, Y., and Wang, G.: Gas-to-Aerosol Phase Partitioning of Atmospheric Water-
691 Soluble Organic Compounds at a Rural Site in China: An Enhancing Effect of NH₃ on SOA
692 Formation, *Environ. Sci. Technol.*, 56, 3915-3924, 10.1021/acs.est.1c06855, 2022.
- 693 Martinelli, L. A., Camargo, P. B., Lara, L., Victoria, R. L., and Artaxo, P.: Stable carbon and nitrogen
694 isotopic composition of bulk aerosol particles in a C4 plant landscape of southeast Brazil, *Atmos.*
695 *Environ.*, 36, 2427-2432, 10.1016/s1352-2310(01)00454-x, 2002.
- 696 Meng, J., Wang, G., Hou, Z., Liu, X., Wei, B., Wu, C., Cao, C., Wang, J., Li, J., Cao, J., Zhang, E.,
697 Dong, J., Liu, J., Ge, S., and Xie, Y.: Molecular distribution and stable carbon isotopic



- 698 compositions of dicarboxylic acids and related SOA from biogenic sources in the summertime
699 atmosphere of Mt. Tai in the North China Plain, *Atmos. Chem. Phys.*, 18, 15069-15086,
700 10.5194/acp-18-15069-2018, 2018.
- 701 Mo, Y., Li, J., Cheng, Z., Zhong, G., Zhu, S., Tian, C., Chen, Y., and Zhang, G.: Dual carbon isotope-
702 based source apportionment and light absorption properties of water-soluble organic carbon in
703 PM_{2.5} over China, *J. Geophys. Res.: Atmos.*, e2020JD033920,
704 <https://doi.org/10.1029/2020JD033920>, 2021.
- 705 Myriokefalitakis, S., Tsigaridis, K., Mihalopoulos, N., Sciare, J., Nenes, A., Kawamura, K., Segers,
706 A., and Kanakidou, M.: In-cloud oxalate formation in the global troposphere: a 3-D modeling
707 study, *Atmos. Chem. Phys.*, 11, 5761-5782, 10.5194/acp-11-5761-2011, 2011.
- 708 Pavuluri, C. M. and Kawamura, K.: Evidence for ¹³C-enrichment in oxalic acid via iron
709 catalyzed photolysis in aqueous phase, *Geophys. Res. Lett.*, 39, n/a-n/a, 10.1029/2011gl050398,
710 2012.
- 711 Pavuluri, C. M., Kawamura, K., and Swaminathan, T.: Water-soluble organic carbon, dicarboxylic
712 acids, ketoacids, and α -dicarbonyls in the tropical Indian aerosols, *J. Geophys. Res.: Atmos.*, 115,
713 10.1029/2009jd012661, 2010.
- 714 Pavuluri, C. M., Kawamura, K., Swaminathan, T., and Tachibana, E.: Stable carbon isotopic
715 compositions of total carbon, dicarboxylic acids and glyoxylic acid in the tropical Indian
716 aerosols: Implications for sources and photochemical processing of organic aerosols, *J.*
717 *Geophys. Res.: Atmos.*, 116, 10.1029/2011jd015617, 2011.
- 718 Qi, W., Wang, G., Dai, W., Liu, S., Zhang, T., Wu, C., Li, J., Shen, M., Guo, X., Meng, J., and Li,
719 J.: Molecular characteristics and stable carbon isotope compositions of dicarboxylic acids and
720 related compounds in wintertime aerosols of Northwest China, *Sci. Rep.*, 12, 11266,
721 10.1038/s41598-022-15222-6, 2022.
- 722 Qiu, X., Duan, L., Chai, F., Wang, S., Yu, Q., and Wang, S.: Deriving High-Resolution Emission
723 Inventory of Open Biomass Burning in China based on Satellite Observations, *Environ. Sci.*
724 *Technol.*, 50, 11779-11786, 10.1021/acs.est.6b02705, 2016.
- 725 Shen, M., Ho, K. F., Dai, W., Liu, S., Zhang, T., Wang, Q., Meng, J., Chow, J. C., Watson, J. G.,
726 Cao, J., and Li, J.: Distribution and stable carbon isotopic composition of dicarboxylic acids,
727 ketocarboxylic acids and α -dicarbonyls in fresh and aged biomass burning
728 aerosols, *Atmos. Chem. Phys.*, 22, 7489-7504, 10.5194/acp-22-7489-2022, 2022.
- 729 Smith, B. N. and Epstein, S.: 2 categories of C-13/C-12 ratios for higher plants, *Plant Physiol.*, 47,
730 380-384, 10.1104/pp.47.3.380, 1971.
- 731 Szidat, S., Jenk, T. M., Sinal, H. A., Kalberer, M., Wacker, L., Hajdas, I., Kasper-Giebl, A., and
732 Baltensperger, U.: Contributions of fossil fuel, biomass-burning, and biogenic emissions to
733 carbonaceous aerosols in Zurich as traced by C-14, *J. Geophys. Res.: Atmos.*, 111,
734 10.1029/2005jd006590, 2006.
- 735 Szidat, S., Jenk, T. M., Gaggeler, H. W., Sinal, H. A., Fisseha, R., Baltensperger, U., Kalberer, M.,
736 Samburova, V., Wacker, L., Saurer, M., Schwikowski, M., and Hajdas, I.: Source apportionment
737 of aerosols by C-14 measurements in different carbonaceous particle fractions, *Radiocarbon*,
738 46, 475-484, 10.1017/s0033822200039783, 2004.
- 739 van Pinxteren, D., Neusüß, C., and Herrmann, H.: On the abundance and source contributions of



- 740 dicarboxylic acids in size-resolved aerosol particles at continental sites in central Europe, *Atmos.*
741 *Chem. Phys.*, 14, 3913-3928, 10.5194/acp-14-3913-2014, 2014.
- 742 Wang, J., Wang, G., Wu, C., Li, J., Cao, C., Li, J., Xie, Y., Ge, S., Chen, J., Zeng, L., Zhu, T., Zhang,
743 R., and Kawamura, K.: Enhanced aqueous-phase formation of secondary organic aerosols due
744 to the regional biomass burning over North China Plain, *Environ. Pollut.*, 256, 113401,
745 <https://doi.org/10.1016/j.envpol.2019.113401>, 2020.
- 746 Wang, J., Ye, J., Zhang, Q., Zhao, J., Wu, Y., Li, J., Liu, D., Li, W., Zhang, Y., Wu, C., Xie, C., Qin,
747 Y., Lei, Y., Huang, X., Guo, J., Liu, P., Fu, P., Li, Y., Lee, H. C., Choi, H., Zhang, J., Liao, H.,
748 Chen, M., Sun, Y., Ge, X., Martin, S. T., and Jacob, D. J.: Aqueous production of secondary
749 organic aerosol from fossil-fuel emissions in winter Beijing haze, *Proc. Natl Acad. Sci. USA*,
750 118, e2022179118, 10.1073/pnas.2022179118 %J Proceedings of the National Academy of
751 Sciences, 2021.
- 752 Warneck, P.: In-cloud chemistry opens pathway to the formation of oxalic acid in the marine
753 atmosphere, *Atmos. Environ.*, 37, 2423-2427, [https://doi.org/10.1016/S1352-2310\(03\)00136-5](https://doi.org/10.1016/S1352-2310(03)00136-5),
754 2003.
- 755 Widory, D., Roy, S., Le Moullec, Y., Goupil, G., Cocherie, A., and Guerrot, C.: The origin of
756 atmospheric particles in Paris: a view through carbon and lead isotopes, *Atmos. Environ.*, 38,
757 953-961, <https://doi.org/10.1016/j.atmosenv.2003.11.001>, 2004.
- 758 Wu, Z., Wang, Y., Tan, T., Zhu, Y., Li, M., Shang, D., Wang, H., Lu, K., Guo, S., Zeng, L., and
759 Zhang, Y.: Aerosol liquid water driven by anthropogenic inorganic salts: implying its key role
760 in haze formation over the North China Plain, *Environ. Sci. Technol. Lett.*, 5, 160-166,
761 [10.1021/acs.estlett.8b00021](https://doi.org/10.1021/acs.estlett.8b00021), 2018.
- 762 Xing, J., Lu, X., Wang, S., Wang, T., Ding, D., Yu, S., Shindell, D., Ou, Y., Morawska, L., Li, S.,
763 Ren, L., Zhang, Y., Loughlin, D., Zheng, H., Zhao, B., Liu, S., Smith, K. R., and Hao, J.: The
764 quest for improved air quality may push China to continue its CO₂ reduction beyond the Paris
765 Commitment, *Proc. Natl Acad. Sci. USA*, 117, 29535-29542, 10.1073/pnas.2013297117, 2020.
- 766 Xu, B., Cheng, Z., Gustafsson, Ö., Kawamura, K., Jin, B., Zhu, S., Tang, T., Zhang, B., Li, J., and
767 Zhang, G.: Compound-specific radiocarbon analysis of low molecular weight dicarboxylic
768 acids in ambient aerosols using preparative gas chromatography: method development, *Environ.*
769 *Sci. Technol. Lett.*, 8, 135-141, 10.1021/acs.estlett.0c00887, 2021.
- 770 Xu, B., Zhang, G., Gustafsson, Ö., Kawamura, K., Li, J., Andersson, A., Bikkina, S., Kunwar, B.,
771 Pokhrel, A., Zhong, G., Zhao, S., Li, J., Huang, C., Cheng, Z., Zhu, S., Peng, P., and Sheng, G.:
772 Large contribution of fossil-derived components to aqueous secondary organic aerosols in
773 China, *Nat. Commun.*, 13, 5115, 10.1038/s41467-022-32863-3, 2022.
- 774 Yu, Q., Chen, J., Cheng, S., Qin, W., Zhang, Y., Sun, Y., and Ahmad, M.: Seasonal variation of
775 dicarboxylic acids in PM_{2.5} in Beijing: Implications for the formation and aging processes of
776 secondary organic aerosols, *Sci. Total Environ.*, 763, 142964,
777 <https://doi.org/10.1016/j.scitotenv.2020.142964>, 2021.
- 778 Zhang, G., Liu, J., Li, J., Li, P., Wei, N., and Xu, B.: Radiocarbon isotope technique as a powerful
779 tool in tracking anthropogenic emissions of carbonaceous air pollutants and greenhouse gases:
780 A review, *Fundam. Res.*, 1, 306-316, <https://doi.org/10.1016/j.fmre.2021.03.007>, 2021.
- 781 Zhang, Y.-L., Kawamura, K., Cao, F., and Lee, M.: Stable carbon isotopic compositions of low-



782 molecular-weight dicarboxylic acids, oxocarboxylic acids, α -dicarbonyls, and fatty acids:
783 Implications for atmospheric processing of organic aerosols, *J. Geophys. Res.: Atmos.*, 121,
784 3707-3717, 10.1002/2015jd024081, 2016.

785 Zhang, Y.-L., Schnelle-Kreis, J., Abbaszade, G., Zimmermann, R., Zotter, P., Shen, R.-r., Schaefer,
786 K., Shao, L., Prevot, A. S. H., and Szidat, S.: Source Apportionment of Elemental Carbon in
787 Beijing, China: Insights from Radiocarbon and Organic Marker Measurements, *Environ. Sci.*
788 *Technol.*, 49, 8408-8415, 10.1021/acs.est.5b01944, 2015.

789 Zhang, Y., Ren, H., Sun, Y., Cao, F., Chang, Y., Liu, S., Lee, X., Agrios, K., Kawamura, K., Liu, D.,
790 Ren, L., Du, W., Wang, Z., Prévôt, A. S. H., Szidat, S., and Fu, P.: High Contribution of
791 Nonfossil Sources to Submicrometer Organic Aerosols in Beijing, China, *Environ. Sci. Technol.*,
792 51, 7842-7852, 10.1021/acs.est.7b01517, 2017.

793 Zhao, B., Zheng, H., Wang, S., Smith, K. R., Lu, X., Aunan, K., Gu, Y., Wang, Y., Ding, D., Xing,
794 J., Fu, X., Yang, X., Liou, K.-N., and Hao, J.: Change in household fuels dominates the decrease
795 in $PM_{2.5}$ exposure and premature mortality in China in 2005–2015, *Proc. Natl*
796 *Acad. Sci. USA*, 115, 12401-12406, 10.1073/pnas.1812955115 %J Proceedings of the National
797 Academy of Sciences, 2018.

798 Zhao, S., Tian, L., Zou, Z., Liu, X., Zhong, G., Mo, Y., Wang, Y., Tian, Y., Li, J., Guo, H., and Zhang,
799 G.: Probing Legacy and Alternative Flame Retardants in the Air of Chinese Cities, *Environ. Sci.*
800 *Technol.*, 10.1021/acs.est.0c07367, 2021.

801 Zhu, S., Ding, P., Wang, N., Shen, C., Jia, G., and Zhang, G.: The compact AMS facility at
802 Guangzhou Institute of Geochemistry, Chinese Academy of Sciences, *Nucl. Instrum. Methods*
803 *Phys. Res., Sect. B*, 361, 72-75, 10.1016/j.nimb.2015.06.040, 2015.

804